NUREG/CR-6885
LA-UR-04-5416

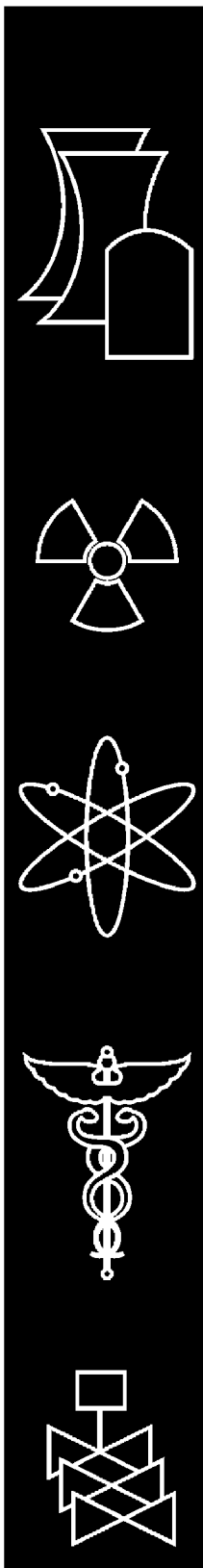

Screen Penetration Test Report

Los Alamos National Laboratory

U.S. Nuclear Regulatory Commission
Office of Nuclear Regulatory Research
Washington, DC 20555-0001

NUREG/CR-6885
LA-UR-04-5416

Screen Penetration Test Report

Manuscript Completed: September 2005
Date Published: October 2005

Principal Investigators: C.B. Dale and B.C. Letellier
Los Alamos National Laboratory
Los Alamos, NM 87545

Prepared by
A. Maji, K. Howe, and F. Carles
University of New Mexico
Department of Civil Engineering
Albuquerque, NM 87110

Tsun-Yung Chang, NRC Project Manager

Prepared for
Division of Engineering Technology
Office of Nuclear Regulatory Research
U.S. Nuclear Regulatory Commission
Washington, DC 20555-0001
NRC Job Code Y6041

Page intentionally left blank

ABSTRACT

The concern raised by Generic Safety Issue (GSI-191), "Assessment of Debris Accumulation on PWR Sump Performance," is the transport of debris to pressurized-water-reactor (PWR) sump screens following a loss-of-coolant accident (LOCA) and subsequent impact to emergency-core-cooling systems (ECCS) and containment-spray systems during recirculation. This document describes the first in a series of tests being conducted to address the effects of debris downstream of the ECCS sump screens. ECCS intake systems have been designed to screen out large post-LOCA debris materials. However, small-sized debris can penetrate these intake strainers or screens and reach critical components of the high-pressure safety injection system, such as pumps and throttle valves.

This report addresses the propensity of different types of insulation debris [fibrous, particulate, and reflective metallic insulation (RMI)] to penetrate PWR sump screens. The variables under consideration include the size of screen openings; the size, shape, and type of debris; the flow velocity upstream of the screen; and the manner in which the debris reaches the screen (on the floor or in the flow). The test matrix consists of 44 tests using combinations of representative screen-opening sizes of 1/4 in., 1/8 in., and 1/16 in. and debris sizes and shapes. Insulation debris consisting of NUKON^{TM} fiberglass, calcium silicate (CalSil), and stainless-steel RMI was tested individually within a linear hydraulic flume. Approach velocities ranged from 0.2 to 1.0 ft/s. These velocities are representative of containment pool approach velocities at the sump screen for current designs, but modifications in many plants may result in lower approach velocities.

Debris screen penetration depends to some extent on all of the test variables examined: screen size; debris size, shape, and type; flow velocity; and method of introduction (on the floor versus in the flow). The debris type determines the relative importance of the remaining test variables. Under certain conditions, results indicate the potential for significant debris screen penetration. It was observed that a significant amount of particulate CalSil insulation (up to 70% in some cases) can pass through a screen opening of any size. Higher flow velocities cause large CalSil clumps to break up, allowing more CalSil to be transported to and pass through the sump screen. A significant amount of fibrous NUKON^{TM} debris (up to 90% in some cases) arriving at the screen in finely separated fibers can pass through the screens. However, if the NUKON^{TM} debris arrives at the screen in larger, agglomerated pieces, only a small amount (<5%) may pass through the screens. Last, when RMI debris was introduced on the floor, the RMI tended to remain stationary on the floor and not transport to the screen. The result was that <22% of the RMI introduced on the floor passed through the screen for all tests. However, a significant percentage (up to 75%) of the RMI passed through the screen when the RMI was introduced directly into the flow immediately before the test screen.

The results presented are applicable to the determination of the effect of the debris that passes through the sump screen on downstream components, such as high-pressure safety injection system pumps and throttle valves. These effects are being investigated in ongoing research at the University of New Mexico, using debris sizes and shapes that can penetrate the screen, as demonstrated by this testing.

Page intentionally left blank

FOREWORD

On September 13, 2004, the U.S. Nuclear Regulatory Commission (NRC) issued Generic Letter (GL) 2004-02, "Potential Impact of Debris Blockage on Emergency Recirculation During Design Basis Accidents at Pressurized-Water-Reactors (PWRs)." In that generic letter, the NRC requested that all PWR licensees perform an evaluation and ensure acceptable performance of their plants' emergency core cooling and containment spray systems during sump recirculation following a loss-of-coolant accident. Toward that end, GL 2004-02 addressed technical issues associated with Generic Safety Issue (GSI-191), "Assessment of Debris Accumulation on PWR Sump Performance," which the NRC established to assess this issue. As part of the evaluation, the generic letter requested that licensees consider how debris that passes through the sump screen affects the performance of equipment downstream of the screen, such as the high-pressure safety injection (HPSI) throttle valves, pumps, piping, heat exchangers, and reactor vessel internals.

This report documents an NRC-sponsored experimental research project, conducted by the University of New Mexico under the supervision of Los Alamos National Laboratory. The primary objective of this study was to develop test data for use in assessing the potential for PWR insulation debris to pass through passive sump screens as a function of debris type, debris size, screen opening size, flow velocity at the screen, and location where the debris reaches the screen (along the floor or in the flow). The test matrix consists of 44 tests using combinations of representative screen opening sizes (1/4", 1/8", and 1/16") and various debris sizes and shapes. Insulation debris consisting of NUKON^{TM} fiberglass, calcium silicate (CalSil), and stainless steel reflective metallic insulation (RMI) were individually tested within a linear hydraulic flume. The effect of the approach velocity was also considered by conducting tests ranging from 0.2 ft/s to 1.0 ft/s. These velocities are representative of sump pool approach velocities at the sump screen for current designs, but modifications in many plants may result in lower approach velocities.

Tests showed that the fraction of debris that penetrates the screens can range from trivial to significant amounts depending on the specific test variable combinations. In particular, the tests showed that virtually all CalSil insulation particulates can pass through any size screen opening. Higher flow velocity breaks up larger CalSil clumps, thereby allowing more total CalSil to transport to and pass through the sump screen. For example, close to 70 percent of the CalSil passed through a 1/4" screen opening in the test conducted at an approach velocity of 0.5 ft/s. A significant amount of NUKON^{TM} debris arriving in finely separated fibers can also pass through the screens. For example, up to 90 percent of NUKON^{TM} passed through a 1/4" screen opening in the test using an approach velocity of 0.5 ft/s. However, if the NUKON^{TM} debris arrives in larger, agglomerated pieces, only a small amount may pass through the screens. For example, less than 5 percent of the larger NUKON^{TM} bundles passed through a 1/4" opening size in the test using an approach velocity of 1 ft/s. In addition, less than 15 percent of RMI debris passed through the screen in tests in which the debris was transported to the screen along the floor and was approximately the same size as the screen opening. More RMI debris (up to 20 percent) passed through the screen in tests in which the debris was smaller than the screen opening. However, a significant percentage (up to 75 percent) of the RMI penetrated the screen in tests in which the debris was smaller than the screen opening and was introduced directly into the flow instead of being transported along the floor.

Consistent with the primary objective of this study, this report provides test data to support performance assessments of HPSI and other components downstream of the sump strainer screen, as they relate to ingested debris. Specifically, NRC staff can use knowledge gained from this study when evaluating licensee responses to GL 2004-02. A follow-on NRC-sponsored study is underway to assess the effect of ingested debris on the operation of HPSI throttle valves downstream of the sump screen.

Carl J. Paperiello, Director
Office of Nuclear Regulatory Research
U.S. Nuclear Regulatory Commission

This page intentionally left blank.

CONTENTS

FIGURES

TABLES

Page

EXECUTIVE SUMMARY

This report describes a series of experiments that was performed in support of resolution of Generic Safety Issue (GSI-191), "Assessment of Debris Accumulation on PWR Sump Performance." These experiments were conducted under the direction of Los Alamos National Laboratory (LANL) in facilities operated by the Civil Engineering Department of the University of New Mexico.

The concern raised by GSI-191 is the transport of debris to pressurized-water-reactor (PWR) sump screens following a loss-of-coolant accident and subsequent impact to emergency-core-cooling and containment-spray systems during recirculation. This study is the first step in evaluating the impact of debris on components downstream from the sump screens, such as the high-pressure safety injection (HPSI) throttle valves and pumps. The results of this report provide test data to support the assessment of PWR sump screen debris penetration.

This report addresses the propensity of different types of insulation debris [fibrous, particulate, and reflective-metallic-insulation (RMI)] to penetrate PWR sump screens with different size openings. The variables under consideration include the size of screen openings, the size and shape of different types of debris, the flow velocity across the screen; and how the debris reaches the screen (on the floor or in the flow). The test matrix consists of 44 tests using combinations of representative screen-opening sizes of 1/4 in., 1/8 in., and 1/16 in. and debris sizes and shapes. Insulation debris consisting of NUKON™ fiberglass, calcium silicate (CalSil), and stainless-steel RMI was tested individually within a linear hydraulic flume. Approach velocities ranged from 0.2 to 1.0 ft/s. These velocities are representative of containment pool approach velocities at the sump screen for current designs, but modifications in many plants may result in lower approach velocities.

The primary purpose of this series of experiments was to establish the basic phenomena of debris penetration. As such, this study was conducted parametrically. Replicate tests were not conducted to understand the uncertainty associated with the test results at any single condition. Rather, single tests were conducted over an appropriate range for the principal variables to understand important factors that contribute to debris bypassing the screen.

The significant finding of this study is that the debris screen penetration depends on all of the variables considered: screen size; debris size, shape, and type; flow velocity; and method of introduction (on the floor versus in the flow). Results show that the fraction of debris that can penetrate the screens ranges from trivial to significant, depending on the combination of variables. It was observed that a significant amount of particulate CalSil insulation (up to 70% in some cases) can pass through a screen opening of any size that was tested. Higher flow velocities cause large CalSil clumps to break up, allowing more CalSil to be transported to and pass through the sump screen. A significant amount of fibrous NUKON™ debris (up to 90% in some cases) arriving at the screen in finely separated fibers can pass through the screens. However, if the NUKON™ debris arrives at the screen in larger, agglomerated pieces, only a small amount (<5%) may pass through the screens. Last, when RMI debris was introduced on the floor, the RMI tended to remain stationary on the floor and not transport to the screen. The result was that <22% of the RMI introduced on the floor passed through the screen for all tests. However, a significant percentage (up to 75%) of the RMI passed through the screen when the RMI was introduced directly into the flow immediately before the test screen.

The experiments reported here indicate that the extent of debris screen penetration depends on the specific combination of test variables. These results are applicable to the determination of the effect of the debris that passes through the sump screen on downstream components, such as HPSI system pumps, HPSI throttle valves, piping, heat exchangers, and reactor vessel internals. These effects are being investigated in ongoing research at the University of New Mexico.

Page intentionally left blank

ABBREVIATIONS

BP	Blender Processed
CalSil	Calcium Silicate
ECCS	Emergency-Core-Cooling System
GSI	Generic Safety Issue
HPSI	High-Pressure Safety Injection
LANL	Los Alamos National Laboratory
LOCA	Loss-of-Coolant Accident
LPSI	Low-Pressure Safety Injection
LS	Leaf Shredded
NRC	Nuclear Regulatory Commission
PVC	Polyvinyl Chloride
PWR	Pressurized-Water Reactor
RMI	Reflective Metallic Insulation
US	United States

Page intentionally left blank

1.0 INTRODUCTION

In the event of a loss-of-coolant accident (LOCA) within the containment of a pressurized water reactor (PWR), piping, thermal insulation, and other materials in the vicinity of the break will be dislodged by break-jet impingement. A fraction of this dislodged insulation will be transported to the containment floor by the steam/water flows induced by the break and the containment sprays. Some of this debris eventually may be transported to and accumulate on the suction sump screens of the emergency-core-cooling system (ECCS) pumps, or debris may pass through the screens. Generic Safety Issue (GSI) 191 is concerned both with (1) debris accumulation on the PWR sump screen and possible loss of ECCS pump net-positive suction head and (2) the possibility that ingested debris could unacceptably degrade ECCS performance.

Since 1999, Los Alamos National Laboratory (LANL) has been supporting the United States (US) Nuclear Regulatory Commission (NRC) in the resolution of GSI 191. Among the research previously completed by LANL is the experimental determination of transport, accumulation, and head loss across a PWR sump screen for flow conditions that are representative of those expected during ECCS recirculation and for debris types and quantities that may accumulate on the screen during a LOCA [1–3]. This study addresses the potential for insulation debris to pass though prototypical sump screens and to pose a threat to components downstream of the sump screen.

The ECCS intake systems have been designed to screen out large post-LOCA debris materials. However, small-sized debris can penetrate these intake strainers or screens and reach critical components. Previous surveys [4] indicate that the ECCS sump screen mesh size can vary from as small as 1/16 in. to as large as 3/4 in. It is possible that smaller-sized or irregularly shaped debris, such as fiberglass, may pass through a mesh opening and then potentially cause blockage or wear, affect heat transfer, or otherwise degrade the operation of critical ECCS components. Prior NRC-sponsored evaluations of possible debris and gas ingestion into ECCS pumps and attendant impacts on pump performance were performed in the early 1980s [5]. However, since this time, the characteristics of LOCA-generated debris are better known. Follow-on work to this initial study examines the potential for debris obstruction to occur for one particular downstream component, the high-pressure safety-injection (HPSI) throttle valve, under various combinations of debris composition, mass loading, and flow duration.

This report presents the findings from a series of sump screen penetration tests for prototypical sump screen/debris combinations. A brief discussion of the test facility (Section 2.0) is followed by a description of debris specimen preparation techniques (Section 3.0). The experimental procedure (Section 4.0) is provided, along with a copy of the test matrix defining all of the parameter combinations tested. The results (Section 5.0) corresponding to the test matirx are documented in tabular and graphical form, followed by a brief discussion of the conclusions (Section 6.0).

Page intentionally left blank

2.0 TEST FACILITY

The objective of this series of tests is to determine the penetrability of various types of insulation debris through the ECCS sump screens. The primary test apparatus used to conduct the screen-penetration tests is a linear hydraulic flume (Figure 2-1). This facility was designed and used previously as a test apparatus to simulate a variety of flow conditions to study debris-transport phenomena [1]. The flume consists of a sturdy open-top box 6.1 m (20 ft) long, 0.9 m (3 ft) wide, and 1.2 m (4 ft) high, with Plexiglas® side panels for viewing the transport of debris. A schematic of the test facility is shown in Figure 2-2. The primary floor structure of the flume is plywood with a Plexiglas® overlay. The flume rests on two 15-cm (6-in.) by 15-cm (6-in.) aluminum I-beams that, in turn, are supported on a wooden truss.

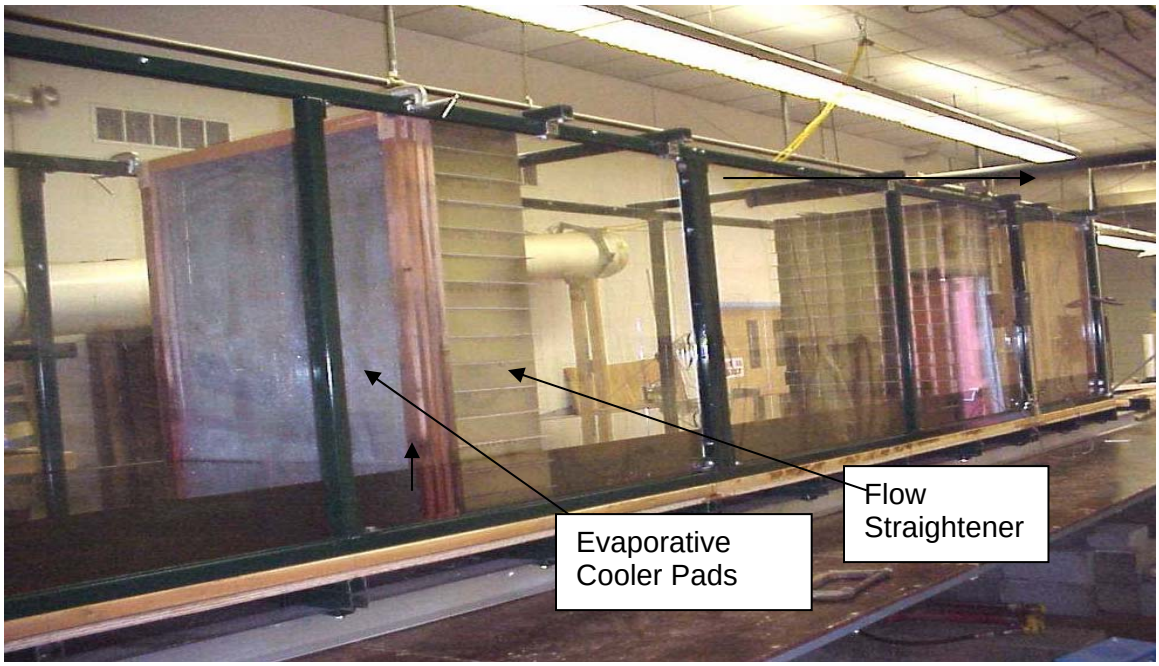

Figure 2-1. Linear flume.

The first 1.2 m (4 ft) of the flume is used for the water inlet and flow-conditioning apparatus. This apparatus consists of a set of evaporative cooler pads that minimize turbulence due to the flow injection and a set of aluminum sheets that straighten the flow (Figure 2-1). The Plexiglas® floor has a surface roughness comparable to an epoxy-coated PWR floor to ensure similar debris transport conditions. Based on research on open-channel hydrology, roughness coefficients of various surfaces are relevant for the quantification of flow. The documented value of the Manning's coefficient, which characterizes the surface roughness of materials for enameled or polymer surfaces (as relevant to an epoxy-coated concrete floor), is ~0.010. This value is also the documented value for Lucite® (similar to Plexiglas®) and other glass-type surfaces. The walls and floor sections are supported structurally with a unistrut steel framework. A variable-speed centrifugal pump capable of 8.35 m^3/min (2200 gpm) is used to pump water from an underground reservoir through overhead piping to fill the test apparatus to the desired level. At the end of each test, water drains out through a 0.305-m (12-in.)-diameter outlet pipe at the opposite end of the flume.

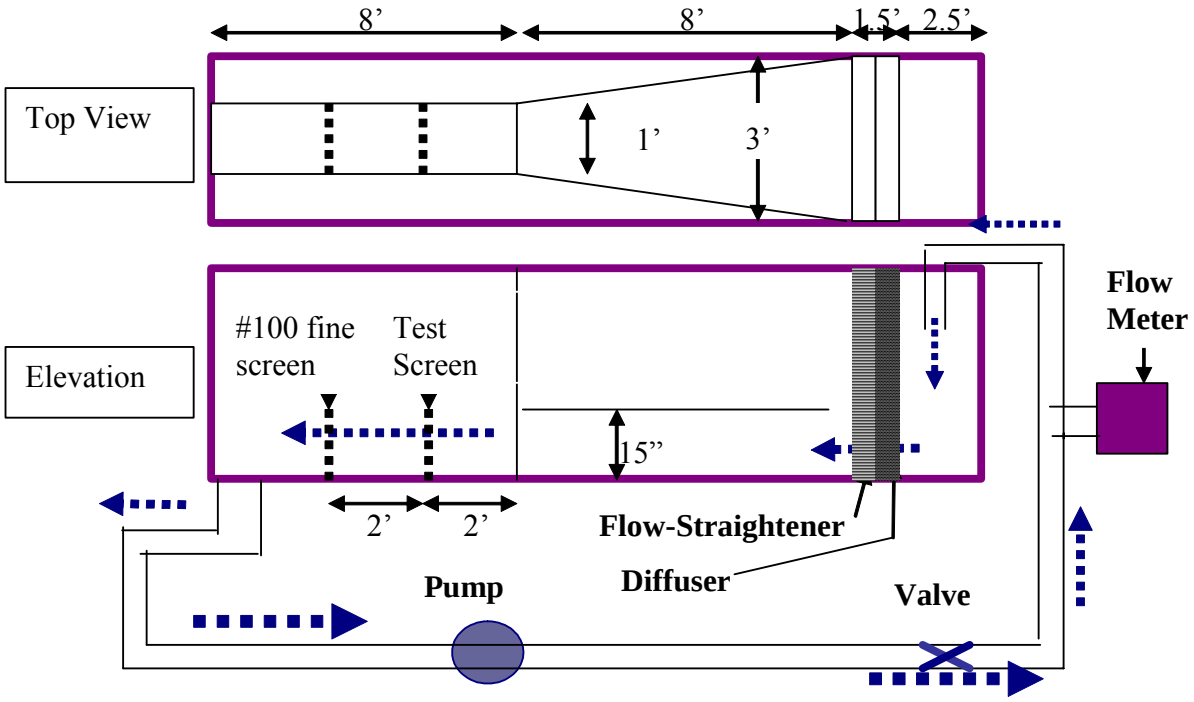

Figure 2-2. Schematic of test facility (not to scale).

To obtain maximum flow velocities at the sump screen, the flow cross section is reduced to force the flow to accelerate by converging the sidewalls. The channel width is decreased linearly from 0.91 m (3 ft) to 0.3 m (1 ft) at the downstream screen over a length of 2.4 m (8 ft). The plywood walls used for flow convergence are shown in Figure 2-3. Downstream from this device, 1.2-m (4-ft)-high Plexiglas® walls confine the flow of water to the central 0.305-m (1-ft) width of the flume (Figure 2-4). Each Plexiglas® wall is held in place by a 5-cm × 10-cm (2-in. × 4-in.) piece of wood at the bottom and by unistrut metal supports at the top. Wooden supports [2.5 cm × 2.5 cm (1 in. × 1 in.)] are placed between the outer walls of the flume and these inner Plexiglas® walls to prevent movement of the walls during the test caused by water pressure and handling of the test equipment. The bottom and side edges of the Plexiglas® are caulked adequately to prevent water leakage during the tests.

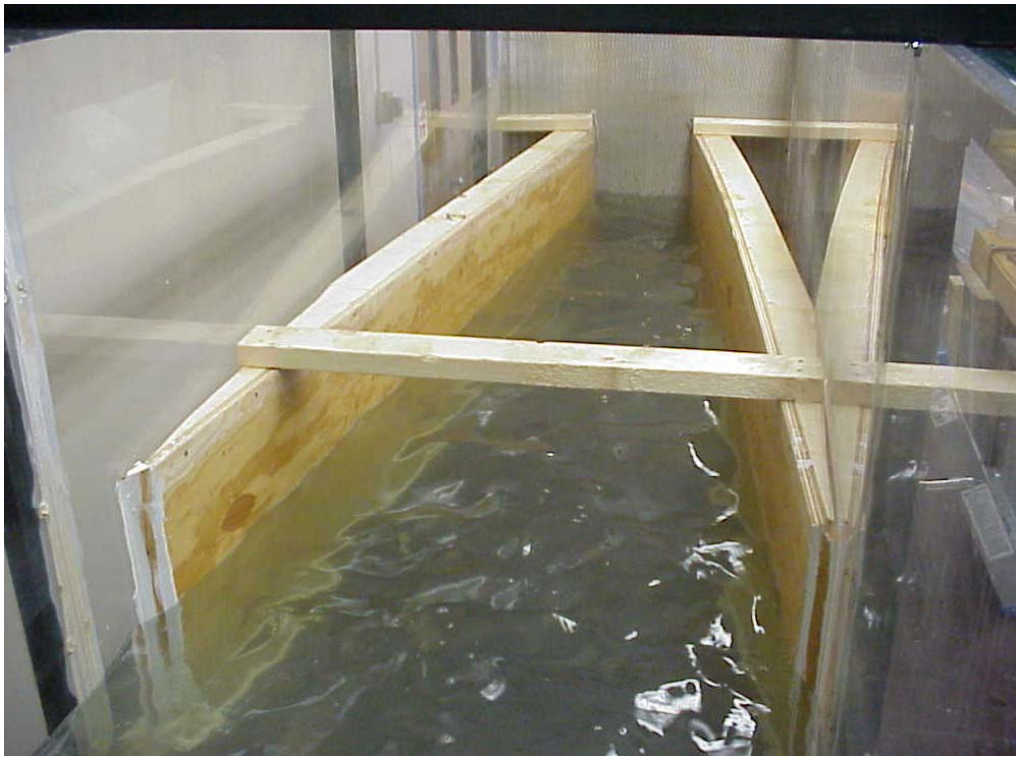

Figure 2-3. Converging flow.

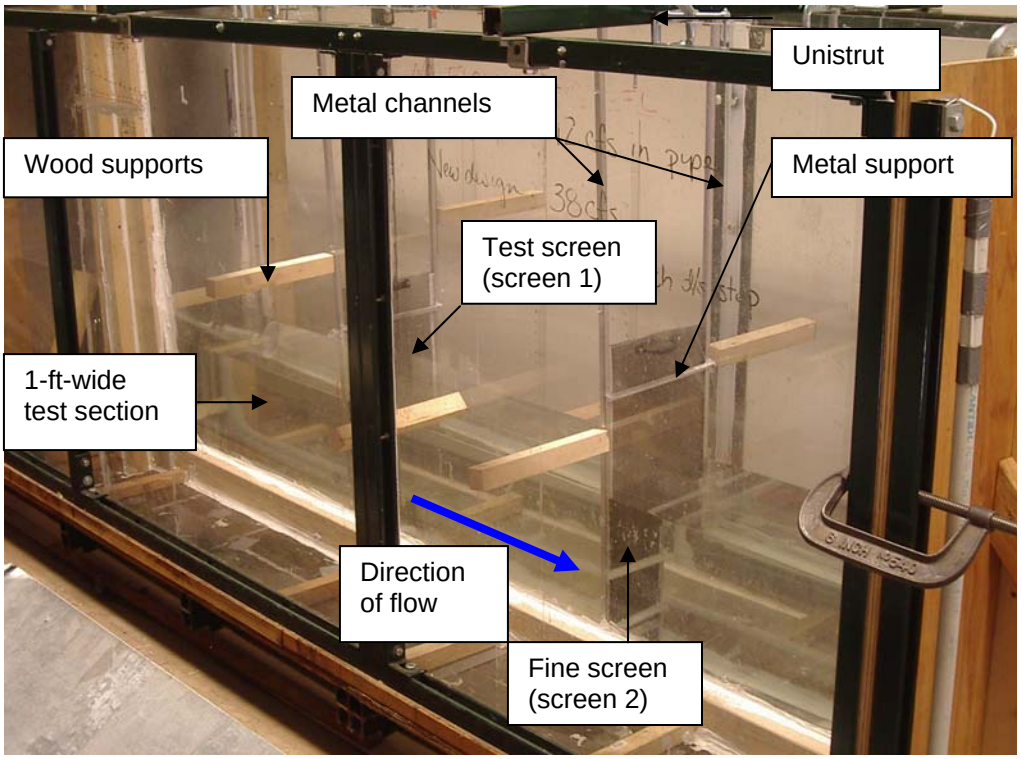

Figure 2-4. Test section [30.48 cm (1 ft) wide] with screens.

A pair of aluminum channels holds the test screen (screen 1) 0.61 m (2 ft) from the end of the converging section. The 0.64-cm (1/4-in.) and 0.32-cm (1/8-in.) square mesh screens can be removed and replaced to allow both weighing of the material embedded on the screens and cleaning. Two horizontal pieces of aluminum channels provide additional support to these screens to prevent bowing due to the pressure of the flowing water. A fine (US-standard #100-sieve) screen (screen 2) is placed further downstream to catch debris that passes through the test screen. The size of openings in this screen is 0.15 mm, with approximately 100 openings per inch (39 openings per centimeter). A coarse, stiff screen with 2.5-cm (1-in.), diamond-shaped openings is attached adhesively to this fine (#100 sieve) screen to provide structural rigidity. A 1.3-cm (~1/2-in.)-high piece of sponge is attached to the bottom of the screens to allow them to seat evenly on the floor, thereby preventing any debris from escaping through the bottom.

Figure 2-5a shows both the test screen and the fine screen located downstream of the test screen, which are used to retain the debris. A close-up of the 0.25-in. test screen is shown in Figure 2-5b. Note that the actual openings on the screen were approximately square in shape and not triangular, as may be incorrectly inferred from this photograph because of the three-dimensional (3D) weave of the wires and the angle at which this photo was taken. Figure 2-5b also shows the horizontal tray on the floor of the flume, which was used to remove and subsequently weigh the debris retained on the floor. A tray was placed on the floor of the test section immediately before each of the two screens. Each tray is 0.305 m (12 in.) wide and 0.41 m (16 in.) long, with a 1.3-cm (~1/2-in.)-high metal edge. Each tray consists of a fine (#200-sieve) screen attached adhesively to a stiffer screen. The size of the openings in the #200 screen is 0.075 mm, with approximately 200 openings per inch (79 openings per centimeter). These screens were removed vertically using attached nylon strings to collect the debris on the floor.

Figure 2-5a. Test screen and fine screen in the test section.

Figure 2-5b. Close-up of the 0.64-cm (0.25-in.)-opening screen and tray on the floor.

Page intentionally left blank

3.0 SPECIMEN PREPARATION

NUKON™, calcium silicate (CalSil), and reflective metallic insulation (RMI) debris specimens were used in these experiments. Preparation of each type of insulation debris was based on previous debris generation experiments [6]. These experiments showed that some of the fibrous debris could be very small (microscopic) in size. The fibrous insulation is coated with a thin layer of organic material, which causes it to float on water for long periods of time. However, this coating is lost after a short exposure to temperatures above 90°C, which is expected to occur in a typical post-LOCA environment. After this coating is lost, the fibrous insulation no longer floats on the surface. Additionally, these studies indicated that a small but significant portion (4.3%) of RMI debris was ≤0.64 cm (1/4 in.) in size. Also, at a target distance of 5 to 11 times the break diameter, the amount of particulate (CalSil) generated by jet impingement was as high as 46% of the amount of CalSil in the zone affected by the jet [6, 7].

The preparation procedure for the NUKON™ and CalSil debris test specimens was identical to previous studies [1, 8]. NUKON™ insulation debris was generated by using a leaf shredder to shred blanket insulation, followed by heating it to >90°C to remove the coating on the surface of the glass fibers, which more accurately simulated post-LOCA fiber conditions. The NUKON™ then was stirred for 5 min using a kitchen blender to separate the fibers and prevent clumping. Figure 3-1 shows the NUKON™ after processing by a leaf shredder (LS NUKON™).

Figure 3-1. LS NUKON™.

The particle-, or clumping-, size distribution of the blender-processed NUKON™ (BP NUKON™), shown in Figure 3-2, has not been determined. Drying the wet BP NUKON™ to obtain a size distribution causes the fibrous debris to stick together, which leads to clumping that is not representative of the characteristics of hydrated NUKON™ under flowing conditions. The CalSil (Figure 3-3) was initially obtained as a mixture of clumps and fine powder. The CalSil was introduced in the experiment as obtained, with no attempt to break up the clumps. To quantify the particle-size distribution, a sample of the dry CalSil was sieved in accordance with the American Society for Testing and Materials international standard D422-63. The results are provided in Table 3-1.

Figure 3-2. BP NUKON™.

The stainless-steel RMI, ~0.5 mm (2 mils) thick, is prepared by cutting foils of the required sizes from a large 2.4-m × 1.2-m (8-ft × 4-ft) rectangular sheet of the material. The RMI insulation is installed in the plants in the form of cassettes ~30.5 cm × 30.5 cm (1 ft^2), as shown in Figure 3-4. Inside the cassettes are thin sheets of stainless steel separated by air gaps. The RMI foil sheet was cut using medium-sized shears, after scribing parallel lines on the RMI sheet to maintain size uniformity. For two different screen openings, 0.64 cm (1/4 in.) and 0.32 cm (1/8 in.), two sizes of flat, square RMI were used. The two sizes of square RMI specimens were equal to the screen opening and to three-fourths of the screen opening. Thus, for the 0.64-cm (1/4-in.) screen opening, the sizes of the RMI debris used were 0.64 cm (1/4 in.) × 0.64 cm (1/4 in.) and 0.48 cm (3/16 in.) × 0.48 cm (3/16 in.). A third size of RMI was introduced solely for the 0.64-cm (1/4-in.) screen opening. This third type of stainless-steel RMI had an aspect ratio of 4:1 [1.27 cm (1/2 in.) × 0.32 cm (1/8 in.) in size].

Figure 3-3. Prototypical crushed CalSil debris.

Table 3-1. Results of Particle Size (Sieve) Analysis of CalSil

Sieve #	Opening (mm)	Mass (g) Retained	% Retained	Cumulative % Retained	% Passing
4	4.75	80.07	40.17	40.17	59.83
10	2	13.95	7.00	47.17	52.83
20	0.85	7.99	4.01	51.18	48.82
100	0.15	48.86	24.51	75.70	24.30
200	0.075	42.53	21.34	97.03	2.97
Pan		5.91	2.97	100.00	0.00
		199.31			

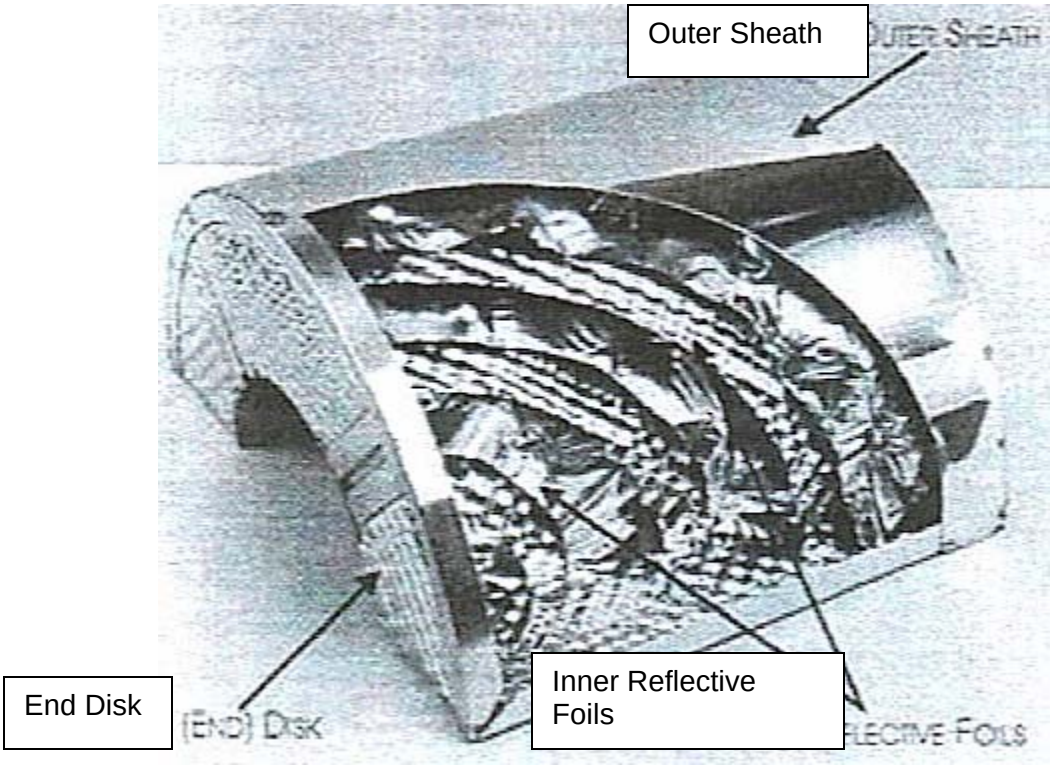

Figure 3-4. Cutout of an RMI cassette.

Fifty pieces each of the 0.635-cm (1/4-in.) and the 0.317-cm (1/8-in.) square RMI were weighed individually on a scale. The average weight of the 0.317-cm (1/8-in.) square pieces was 0.00373 g, with a standard deviation of 0.00068 g. The average weight of the 0.635-cm (1/4-in.) square pieces was 0.01687 g, with a standard deviation of 0.00133 g.

To further quantify the processing variability from cutting the RMI foils, the sides were measured for nine pieces each of 0.317-cm (1/8-in.) square RMI and 0.635-cm (1/4-in.) square RMI. The RMI measurements were made using the Image Processing toolbox in MATLAB®. This process involved taking a digital image of the RMI foils with a scale. With the scale, the pixel size in inches could be determined. The image was then loaded into MATLAB®, where the image was sharpened using the "imadjust" function that then converted to a binary image to better distinguish the edges. After the binary images were created, the pixel locations were found for each corner of the nine samples. With the length of each side in pixels, the conversion to inches was made to determine dimensions in inches. The lengths of the sides of the RMI samples are given in Table 3-2. The results for both foil sizes visually conform to a normal distribution function, with the 0.317-cm (1/8-in.) square RMI foils having a mean of 0.3172 cm (0.1249 in.), with a standard deviation of 0.0257 cm (0.0101 in.), and the 0.635-cm (1/4-in.) square RMI foils having a mean of 0.6642 cm (0.2615 in.), with a standard deviation of 0.0315 cm (0.0124 in.).

Table 3-2. RMI Particle-Size Distribution (Measured in Inches)

0.317-cm (1/8-in.) Square RMI				
Sample #	**Top**	**Right**	**Bottom**	**Left**
1	0.1182	0.1323	0.1288	0.1306
2	0.1288	0.1147	0.1235	0.1147
3	0.1235	0.1306	0.1270	0.1323
4	0.1323	0.1129	0.1306	0.1129
5	0.1464	0.1306	0.1500	0.1288
6	0.1111	0.1217	0.1111	0.1235
7	0.1376	0.1164	0.1376	0.1217
8	0.1253	0.1059	0.1253	0.1094
9	0.1270	0.1200	0.1358	0.1182
			Mean	0.1249
			Stan. dev.	0.0101
0.635-cm (1/4-in.) Square RMI				
Sample #	**Top**	**Right**	**Bottom**	**Left**
1	0.2602	0.2480	0.2602	0.2399
2	0.2684	0.2602	0.2724	0.2521
3	0.2806	0.2684	0.2846	0.2643
4	0.2846	0.2440	0.2765	0.2684
5	0.2480	0.2643	0.2521	0.2724
6	0.2521	0.2684	0.2399	0.2724
7	0.2521	0.2521	0.2602	0.2562
8	0.2765	0.2765	0.2643	0.2684
9	0.2562	0.2562	0.2480	0.2440
			Mean	0.2615
			Stan. dev.	0.0124

Page intentionally left blank

4.0 TEST PROCEDURE

Once the desired water depth [38 cm (15 in.)] was reached in the flume, a 5-hp recirculating pump was used to run the tests in a closed-loop configuration. The flow rate was adjusted using a control valve. With the valve completely open, the maximum flow rate was ~2.28 m^3/min (600 gpm). Based on the measured flow rate, the average flow velocities required for the execution of the tests were established. Water was allowed to recirculate for 5 min before debris was introduced into the flow. This recirculation allowed the flow to reach a steady state and also allowed any extraneous particles to be filtered out of the test section by the diffuser (evaporative cooler pads) at the upstream end of the flume. To ensure that extraneous material did not build up on the fine screen and influence the test results, the fine screen was inserted after the 5 min of recirculation. Observations of the fine screen after this procedure indicated that this time was sufficient to ensure that the fine screen was clean. However, for experiments involving the CalSil dust, these fine particulates passed through the evaporative cooler pads and could have deposited on the fine screen. Therefore, the water in the flume was thrown out after each CalSil test, followed by flushing the system with fresh water before the next test. This procedure was judged to be effective because in the subsequent tests, the water remained visibly clean, with no discernable quantity of CalSil buildup observed on the fine screen.

Insulation debris generally was introduced on the Plexiglas® floor, 0.61 m (2 ft) upstream from the screen through a 15.2-cm (6-in.)-diameter polyvinyl chloride (PVC) pipe. The bottom of this pipe rested on the Plexiglas® floor of the flume; thus, the turbulence and flow in the flume did not influence the debris as it settled inside the pipe. Inside the PVC pipe, the debris settled to the floor over a 2- to 3-min period before the pipe slowly was lifted and the debris was subject to the flow conditions. When introduced in this manner, all of the debris ended up dispersed on the floor. Being almost neutrally buoyant, some of the NUKON™ remained loosely stacked on top of or close to other NUKON™ on the floor. To separate the effect of floor transport from screen penetration (for RMI only), additional tests were conducted by introducing the RMI debris directly into the flow at a distance 15.2 cm (6 in.) from the test screen. To prevent the RMI from floating on the surface because of surface tension forces, the container with the RMI was held under the water for 30 s, during which time the RMI was stirred slowly, before turning the container over to introduce the RMI into the flow.

The flow rate was measured using a Hoffer (model HP-B series) flowmeter calibrated for the 15.2-cm (6-in.)-diameter recirculating pipe. The flowmeter was calibrated initially (traceable to the National Institute of Standards and Technology) at the factory before shipment to a repeatability of 1% of reading over a flow range of 0.285 to 5.7 ft^3/s (125 to 2500 gpm). For the flow rates of interest to this project, the time taken to fill a 151.2-liter (40-gal.) drum was measured with a stopwatch (accurate to 0.1 s) and the results were compared with the flow rate measured by the flowmeter. The flowmeter also was calibrated at the beginning of the test program by measuring the flow velocities at the screen independently with a velocity probe. Each test was performed with ~10 g of debris of each type. This amount was selected to obtain a quantity sufficient to be weighed and yet not enough to cause any significant head loss on the screens. Because one type of debris could influence the penetration of another kind (such as NUKON™ on the screen, thus blocking subsequent penetration of RMI), only one kind of debris was introduced in a given experiment. A study of the combined effects of various debris types was beyond the scope of this research.

The fraction of debris that does not pass through the screens is determined by weighing the amount of debris caught on the test screen and before the test screen on the flat tray. The amount that passes through the screen is measured by carefully removing the material on the fine (#100-sieve) screen downstream and the material between the two screens. To weigh the amount of NUKON™, the fibers must be separated from the water through a slow filtration process (Figure 4-1) before being dried in the oven. Small pieces of RMI that did not move to the trays must be removed by hand (Figure 4-2).

The final test matrix (Table 4-1) reflects initial planning, as well as some revisions based on initial testing results. Revisions were made to ensure that representative debris types and sizes, screen-opening sizes, and flow velocities were used in appropriate combinations. The test matrix velocity range, shown in Table 4-1, was developed initially based on the presumption that most of the NUKON™ and CalSil finer than a certain size will pass through the screens at velocities ≥30.5 cm/s (1 ft/s). Additionally, a survey of the US PWRs indicated that only 25% of the plants are likely to have a sump-screen flow velocity in excess of 30.48 cm/s (1.0 ft/s). The lowest flow velocity used in the test matrix, 6.096 cm/s (0.2 ft/s), corresponds to the velocity at which the stainless-steel RMI begins to move when placed on the floor, as reported in NUREG/CR-6772 (Note: The incipient flow velocity ranges from 1.829–3.658 cm/s (0.06–0.12 ft/s) for NUKON™ and is 7.620 cm/s (0.25 ft/s) for large clumps of CalSil.) [1]. This threshold velocity ensures that debris reaches the test screen. The screen openings of 0.32 cm (1/8 in.) and 0.64 cm (1/4 in.) were selected because the majority of PWR screens have openings of 0.32 cm (1/8 in.) and because most of the remaining PWR screens have openings of 0.64 cm (1/4 in.) [8, 9]. A finer, 0.16-cm (1/16-in.)-opening screen also was used to study how a reduced mesh opening might affect the screen penetration of the LS NUKON™.

Figure 4-1. Filtration of NUKON™ to remove water.

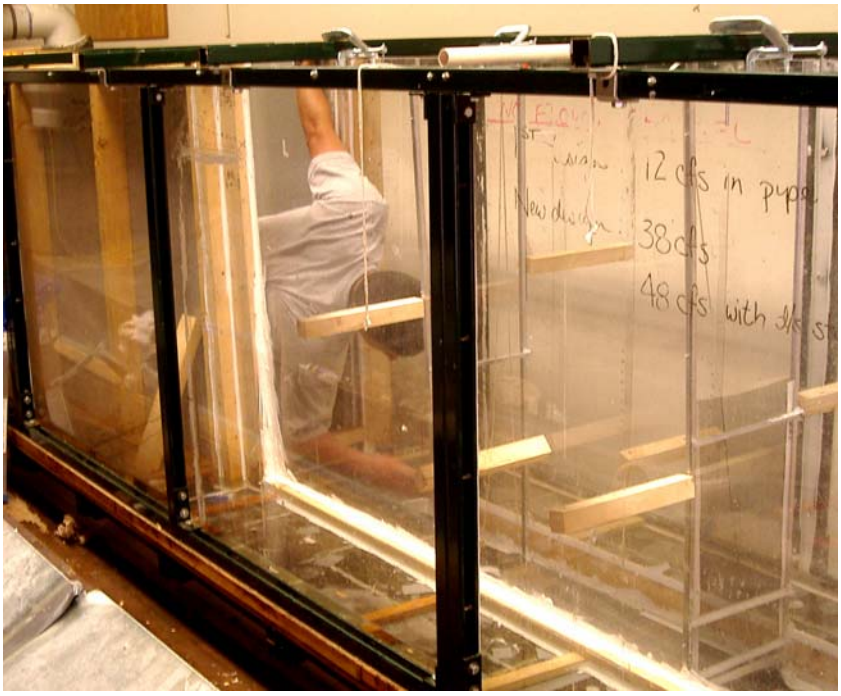

Figure 4-2. Removal of RMI by hand inside the flume.

Table 4-1. Test Matrix

Flow Velocity cm/s (ft/s)	Screen Opening 0.64 cm (1/4 in.)				Screen Opening 0.32 cm (1/8 in.)				Screen Opening 0.16 cm (1/16 in.)
	BP NUKON™	LS NUKON™	CalSil	RMI[a,b]	BP NUKON™	LS NUKON™	CalSil	RMI[b,c]	LS NUKON™
6.096 (0.2)	X	X	X	X	X	X	X	X	X
15.24 (0.5)	X	X	X	X	X	X	X	X	X
30.48 (1.0)		X		X		X		X	X

[a]Two sizes of square RMI and one size of 4:1 aspect-ratio RMI, per Section 3.0.
[b]RMI was introduced both on the floor and in the flow to remove the floor transport component.
[c]Only two sizes of square RMI samples, per Section 3.0.

The size and weight fraction of debris generated by a LOCA were discussed in a previous report [7] and in Section 3.0. To study the effect of the NUKON™ debris size, it was decided to conduct comparison tests between the LS and BP NUKON™ processing techniques. As discussed in Section 3.0, the BP NUKON™ is a more finely separated mixture than LS NUKON™. Because CalSil and NUKON™ reach the screen readily, all of the CalSil and NUKON™ debris was introduced on the floor. Although the initial tests placed RMI on the floor, additional tests were conducted that introduced RMI directly into the flow. The purpose of introducing RMI in the flow is to separate the confounding effects of transport from the screen penetration results. The study of debris transport is not within the scope of this report. A single set of RMI tests was conducted with a 4:1 aspect ratio (Section 3.0). As previously mentioned the RMI pieces were 1.27 cm (1/2 in.) × 0.32 cm (1/8 in.) in size and were used with a 0.64-cm (1/4-in.) test screen. This RMI test was performed solely by introduction in the flow rather than on the floor.

Page intentionally left blank

5.0 TEST RESULTS

Results of the tests identified in Table 4-1 are shown in Tables 5-1 through 5-3. The information is presented as a function of flow velocity, with results broken down by debris type (including method of introduction), screen size, and debris size (or preparation) where appropriate. The measured weights W_0, W_1, and W_2 in Tables 5-1 through 5-3, respectively, represent the total amount of sample introduced, the amount retained on and before the test screen (screen 1), and the amount retained on the fine screen (screen 2) plus the amount between the two screens.

It can be seen from Tables 5-1 through 5-3 that all of the RMI introduced in the test section is accounted for ($W_0 = W_1 + W_2$). However, some of the NUKON™ and a significant percentage of CalSil were not captured by screen 1 or 2 and were not recovered after each test, i.e. $W_0 \geq W_1 + W_2$. This result can be explained (1) for NUKON™ by the fact that it is difficult to collect all of the small fibrous pieces following the test and (2) for CalSil because a significant amount of the fine particles goes through the fine screen and is never recaptured.

The destination of this lost material could be one of three places:

1. before the test screen (drops to the floor or is never entrained),
2. between the two screens (passes through the sump screen but does not transport further), or
3. past the second screen and/or is too fine to capture.

An attempt is made to account for the material from destination 1 by collecting the material from the floor and including it in the W_1 measurement. In a similar manner, material with destination 2 is collected and included with the W_2 measurement. However, for the fine NUKON™ and CalSil debris, this collection process is not sufficient to ensure that all inserted debris is recovered.

Two concerns have been identified for debris impact analyses: head loss across the sump screen and downstream component effects. Two different methods are used to conservatively estimate the percentage of material that passes through the test screen (% passing) to address both concerns. In the context of head loss, it is conservative to maximize what does not pass through the test screen for each experiment by treating all lost material as if it were retained on screen 1. Therefore, the minimum quantity of material passing through the sump screen, "$\%passing_1$," is defined as $(W_2/W_0) \times 100$. In the context of adverse downstream effects, it is conservative to maximize what passes through the sump screen by treating the lost material as if it were retained on screen 2. The maximum quantity of material passing through the sump screen, "$\%passing_2$," is defined as $((W_0 - W_1)/W_0) \times 100$. The difference between these two measurements is equivalent to the percentage of debris that is not recovered after each test.

Table 5-1. Test Results for NUKON™ and CalSil

NUKON™ Fiberglass and Calcium Silicate Insulation															
Velocity cm/s (ft/s)	**Screen Size: 0.64 cm × 0.64 cm (1/4 in. × 1/4 in.)**														
	BP NUKON™					**LS NUKON™**					**CalSil**				
	W_o (g)	**W_1 (g)**	**W_2 (g)**	**%Passing$_1$**	**%Passing$_2$**	**W_o (g)**	**W_1 (g)**	**W_2 (g)**	**%Passing$_1$**	**%Passing$_2$**	**W_o (g)**	**W_1 (g)**	**W_2 (g)**	**%Passing$_1$**	**%Passing$_2$**
6.34 (0.208)	10.25	2.91	6.56	64.00	71.61	10.18	9.91	0.09	0.88	2.65	10.14	5.75	1.27	12.52	43.29
15.64 (0.513)	10.26	0.98	7.75	75.54	90.45	10.18	9.88	0.06	0.59	2.95	10.17	3.29	2.58	25.37	67.65
32.46 (1.065)	--	--	--	--	--	10.18	9.66	0.00	0.00	5.11	--	--	--	--	--
Velocity cm/s (ft/s)	**Screen Size: 0.32 cm × 0.32 cm (1/8 in. × 1/8 in.)**														
	BP NUKON™					**LS NUKON™**					**CalSil**				
	W_o (g)	**W_1 (g)**	**W_2 (g)**	**%Passing$_1$**	**%Passing$_2$**	**W_o (g)**	**W_1 (g)**	**W_2 (g)**	**%Passing$_1$**	**%Passing$_2$**	**W_o (g)**	**W_1 (g)**	**W_2 (g)**	**%Passing$_1$**	**%Passing$_2$**
6.34 (0.208)	10.07	2.06	6.37	63.26	79.54	10.17	9.85	0.06	0.59	3.15	10.01	6.45	0.42	4.20	35.56
15.64 (0.513)	10.36	2.49	6.61	63.80	75.97	10.17	9.76	0.08	0.79	4.03	10.26	3.77	1.93	18.81	63.26
32.46 (1.065)	--	--	--	--	--	10.17	9.72	0.00	0.00	4.42	--	--	--	--	--
Velocity cm/s (ft/s)	**Screen Size: 0.16 cm × 0.16 cm (1/16 in. × 1/16 in.)**														
	BP NUKON™					**LS NUKON™**					**CalSil**				
	W_o (g)	**W_1 (g)**	**W_2 (g)**	**%Passing$_1$**	**%Passing$_2$**	**W_o (g)**	**W_1 (g)**	**W_2 (g)**	**%Passing$_1$**	**%Passing$_2$**	**W_o (g)**	**W_1 (g)**	**W_2 (g)**	**%Passing$_1$**	**%Passing$_2$**
6.34 (0.208)	--	--	--	--	--	10.21	9.81	0.09	0.88	3.92	--	--	--	--	--
15.64 (0.513)	--	--	--	--	--	10.21	9.77	0.11	1.08	4.31	--	--	--	--	--
32.46 (1.065)	--	--	--	--	--	10.21	9.69	0.00	0.00	5.09	--	--	--	--	--

W_0 = Original amount of material.

W_1 = Amount of material retained on the first screen (test screen).

W_2 = Amount of material retained on second screen (fine screen).

%Passing$_1$ = $(W_2/W_o) \times 100$ (minimum penetration).

%Passing$_2$ = $((W_o-W_1)/W_o) \times 100$ (maximum penetration).

-- Indicates test conditions that were not studied.

Table 5-2. Test Results for RMI Introduced on the Floor

Reflective Metal Insulation: Introduced on the Floor															
Velocity cm/s (ft/s)	**Screen Size: 0.64 cm × 0.64 cm (1/4 in. × 1/4 in.)**														
	RMI 0.64 cm × 0.64 cm (1/4 in. × 1/4 in.)					**RMI 0.48 cm × 0.48 cm (3/16 in. × 3/16 in.)**					**RMI 1.27 cm × 0.32 cm (1/2 in. × 1/8 in.)**				
	W_o (g)	**W_1 (g)**	**W_2 (g)**	**%Passing$_1$**	**%Passing$_2$**	**W_o (g)**	**W_1 (g)**	**W_2 (g)**	**%Passing$_1$**	**%Passing$_2$**	**W_o (g)**	**W_1 (g)**	**W_2 (g)**	**%Passing$_1$**	**%Passing$_2$**
6.34 (0.208)	10.05	9.98	0.07	0.70	0.70	10.00	9.79	0.21	2.10	2.10	--	--	--	--	--
15.64 (0.513)	10.02	9.91	0.11	1.10	1.10	10.06	9.76	0.30	2.98	2.98	--	--	--	--	--
32.46 (1.065)	9.98	9.43	0.55	5.51	5.51	10.07	8.21	1.86	18.47	18.47	--	--	--	--	--
Velocity cm/s (ft/s)	**Screen Size: 0.32 cm × 0.32 cm (1/8 in. × 1/8 in.)**														
	RMI 0.32 cm × 0.32 cm (1/8 in. × 1/8 in.)					**RMI 0.24 cm × 0.24 cm (3/32 in. × 3/32 in.)**					**RMI 1.27 cm × 0.32 cm (1/2 in. × 1/8 in.)**				
	W_o (g)	**W_1 (g)**	**W_2 (g)**	**%Passing$_1$**	**%Passing$_2$**	**W_o (g)**	**W_1 (g)**	**W_2 (g)**	**%Passing$_1$**	**%Passing$_2$**	**W_o (g)**	**W_1 (g)**	**W_2 (g)**	**%Passing$_1$**	**%Passing$_2$**
6.34 (0.208)	10.07	10.05	0.02	0.20	0.20	10.05	9.96	0.09	0.90	0.90	--	--	--	--	--
15.64 (0.513)	10.04	9.95	0.09	0.90	0.90	10.02	9.69	0.33	3.29	3.29	--	--	--	--	--
32.46 (1.065)	10.08	8.55	1.53	15.18	15.18	10.07	7.87	2.20	21.85	21.85	--	--	--	--	--

W_0 = Original amount of material.

W_1 = Amount of material retained on the first screen (test screen).

W_2 = Amount of material retained on second screen (fine screen).

%Passing$_1$ = $(W_2/W_o) \times 100$ (minimum penetration).

%Passing$_2$ = $((W_o-W_1)/W_o) \times 100$ (maximum penetration).

-- Indicates test conditions that were not studied.

Table 5-3. Test Results for RMI Introduced in the Flow

Reflective Metal Insulation: Introduced in the Flow															
Velocity cm/s (ft/s)	**Screen Size: 0.64 cm × 0.64 cm (1/4 in. × 1/4 in.)**														
	RMI 0.64 cm × 0.64 cm (1/4 in. × 1/4 in.)					**RMI 0.48 cm × 0.48 cm (3/16 in. × 3/16 in.)**					**RMI 1.27 cm × 0.32 cm (1/2 in. × 1/8 in.)**				
	W_o (g)	**W_1 (g)**	**W_2 (g)**	**%Passing$_1$**	**%Passing$_2$**	**W_o (g)**	**W_1 (g)**	**W_2 (g)**	**%Passing$_1$**	**%Passing$_2$**	**W_o (g)**	**W_1 (g)**	**W_2 (g)**	**%Passing$_1$**	**%Passing$_2$**
6.34 (0.208)	10.05	9.21	0.84	8.36	8.36	10.04	2.62	7.42	73.90	73.90	10.01	8.57	1.44	14.39	14.39
15.64 (0.513)	10.05	8.68	1.37	13.63	13.63	10.04	2.45	7.59	75.60	75.60	10.01	8.52	1.49	14.89	14.89
32.46 (1.065)	10.05	8.33	1.72	17.11	17.11	10.04	3.69	6.35	63.25	63.25	10.01	8.87	1.14	11.39	11.39
Velocity cm/s (ft/s)	**Screen Size: 0.32 cm × 0.32 cm (1/8 in. × 1/8 in.)**														
	RMI 0.32 cm × 0.32 cm (1/8 in. × 1/8 in.)					**RMI 0.24 cm × 0.24 cm (3/32 in. × 3/32 in.)**					**RMI 1.27 cm × 0.32 cm (1/2 in. × 1/8 in.)**				
	W_o (g)	**W_1 (g)**	**W_2 (g)**	**%Passing$_1$**	**%Passing$_2$**	**W_o (g)**	**W_1 (g)**	**W_2 (g)**	**%Passing$_1$**	**%Passing$_2$**	**W_o (g)**	**W_1 (g)**	**W_2 (g)**	**%Passing$_1$**	**%Passing$_2$**
6.34 (0.208)	10.04	9.03	1.01	10.06	10.06	10.00	2.60	7.40	74.00	74.00	--	--	--	--	--
15.64 (0.513)	10.04	8.55	1.49	14.84	14.84	10.00	2.34	7.66	76.60	76.60	--	--	--	--	--
32.46 (1.065)	10.04	7.77	2.27	22.61	22.61	10.00	4.03	5.97	59.70	59.70	--	--	--	--	--

W_0 = Original amount of material.

W_1 = Amount of material retained on the first screen (test screen).

W_2 = Amount of material retained on second screen (fine screen).

%Passing$_1$ = $(W_2/W_o) \times 100$ (minimum penetration).

%Passing$_2$ = $((W_o-W_1)/W_o) \times 100$ (maximum penetration).

-- Indicates test conditions that were not studied.

The results for the NUKON™ debris tests are plotted in Figure 5-1, comparing the maximum penetration (%passing$_2$) for BP NUKON™ and LS NUKON™. The plot in Figure 5-1 illustrates that the lack of blending for the LS NUKON™ had a major impact on the fraction of NUKON™ insulation that passed through any of the screens. Only a very small fraction of the LS NUKON™ went through the screens. The results for NUKON™ indicate that the particle-size distribution of the debris is a larger determining factor of screen penetration than either the screen size or flow velocity for the conditions tested.

Figures 5-2 through 5-4 present photographs of the NUKON™ debris tests. The height indicated in Figures 5-2 and 5-3 represents ~30.48 cm (12 in.) in width, which is equal to the width of the test section. Figure 5-2 shows a small amount of BP NUKON™ remaining on the floor in front of the test screen following the test. Figure 5-3 shows a comparatively larger fraction of the finer-sized BP NUKON™ trapped on the fine screen downstream after passing through the test screen. In Figure 5-4 it can be seen that the individual pieces of LS NUKON™ simply aggregated at the test screen and did not pass through. No difference was noted in the transport of the NUKON debris on the floor between the Plexiglas® section and the test section with the screen on the floor. Any NUKON™ debris that transported went all the way to the test screen.

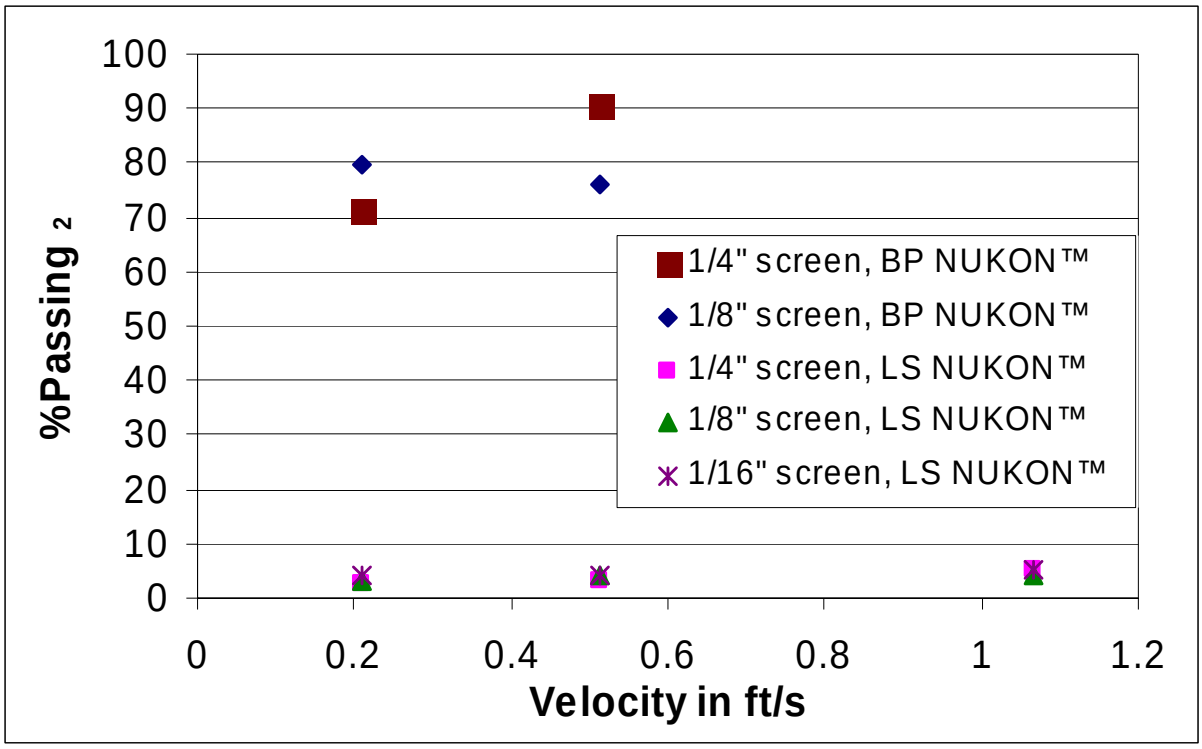

Figure 5-1. NUKON™—%Passing$_2$ (1 ft/s = 0.305 m/s).

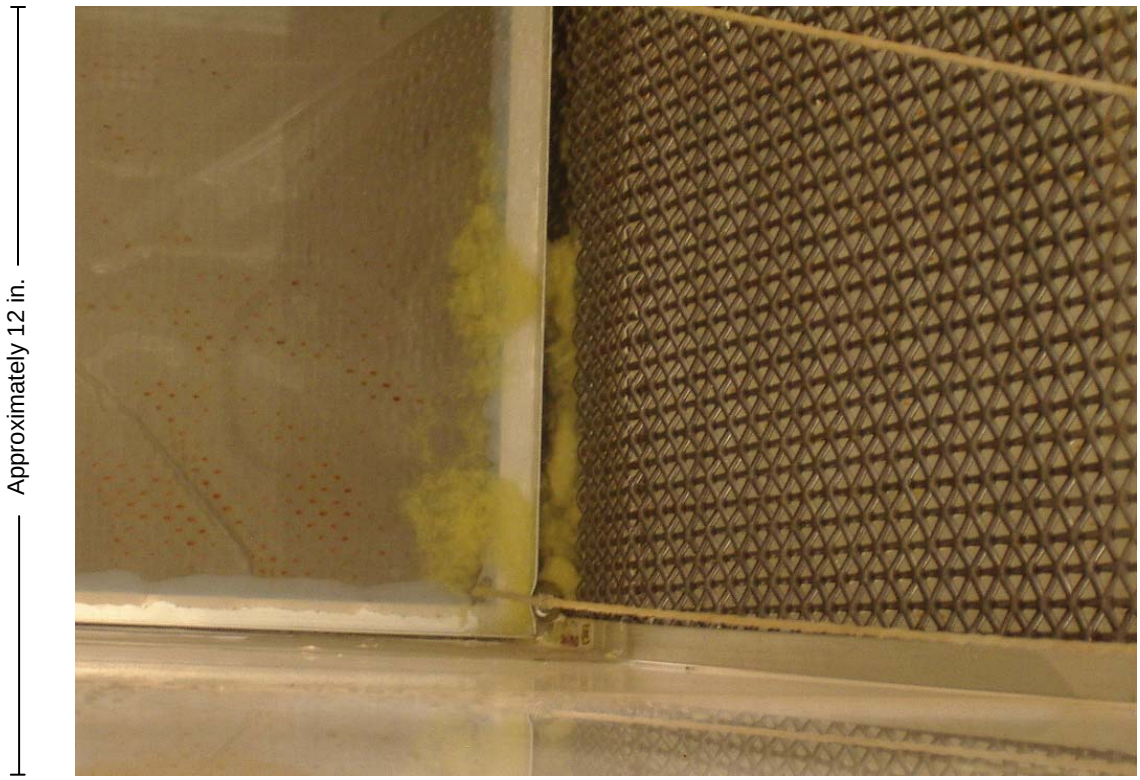

Figure 5-2. Larger pieces of BP NUKON™ on the floor.

Figure 5-3. Finer-sized BP NUKON™ collected on the fine screen located downstream.

Figure 5-4. LS NUKON™ forms clusters at the test screen.

The results for the CalSil debris tests are plotted in Figure 5-5, comparing the minimum and maximum passing percentages. This comparison is made for CalSil because, of all the debris types, the discrepancy between these two measurements is greatest for CalSil. This difference stems from the inability to recover a significant portion of CalSil following the test. Most of the unrecovered CalSil remains suspended in the water and continues to circulate in the loop. A larger fraction of CalSil goes through the test screen than any other debris type. Also, the results show that with a larger screen opening and increasing flow velocity, more of the CalSil passes through, with flow velocity being more important than screen size under the range of conditions tested. The effect of flow velocity largely is due to the increased ability of the flow to break up larger CalSil clumps. The larger clumps of CalSil remain on the floor (Figure 5-6) and do not transport to or are captured by the test screen. Finer clumps and particles disperse in the water (making it murky) and partially collect on the fine screen downstream or on the tray on the floor (Figure 5-7). Some of the larger clumps of CalSil also were caught on the screen of the flat tray immediately before the test screen. Thus, the tray screen's roughness could have affected the CalSil test results.

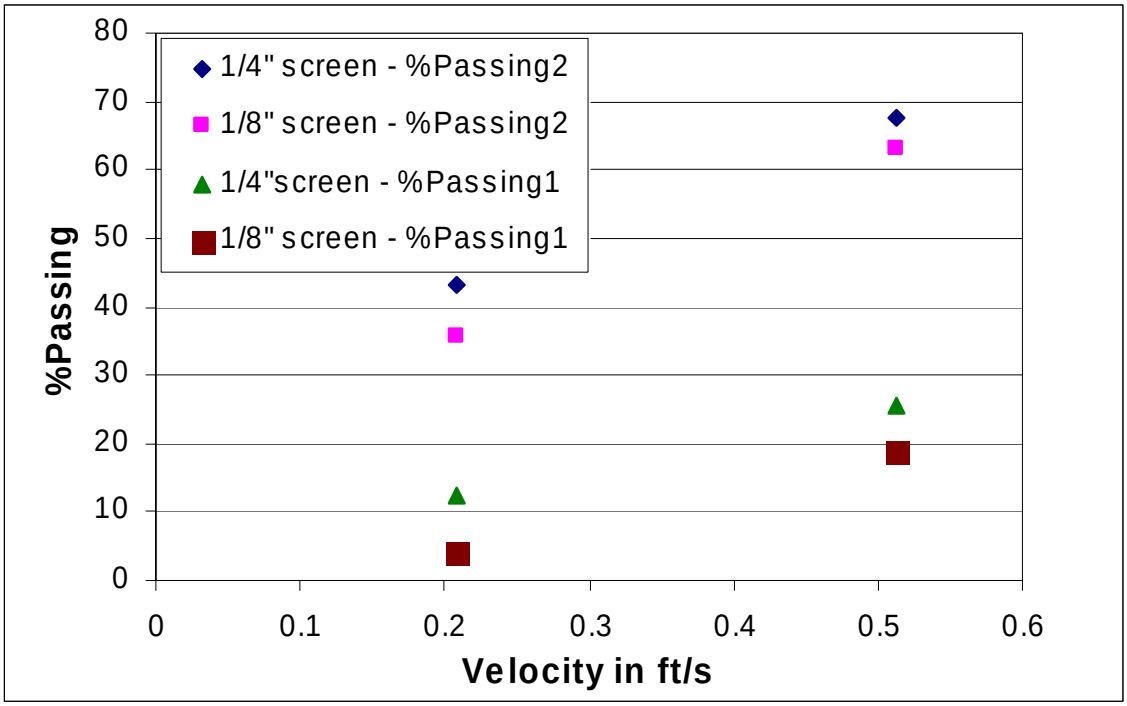

Figure 5-5. CalSil—%Passing (1 ft/s = 0.305 m/s).

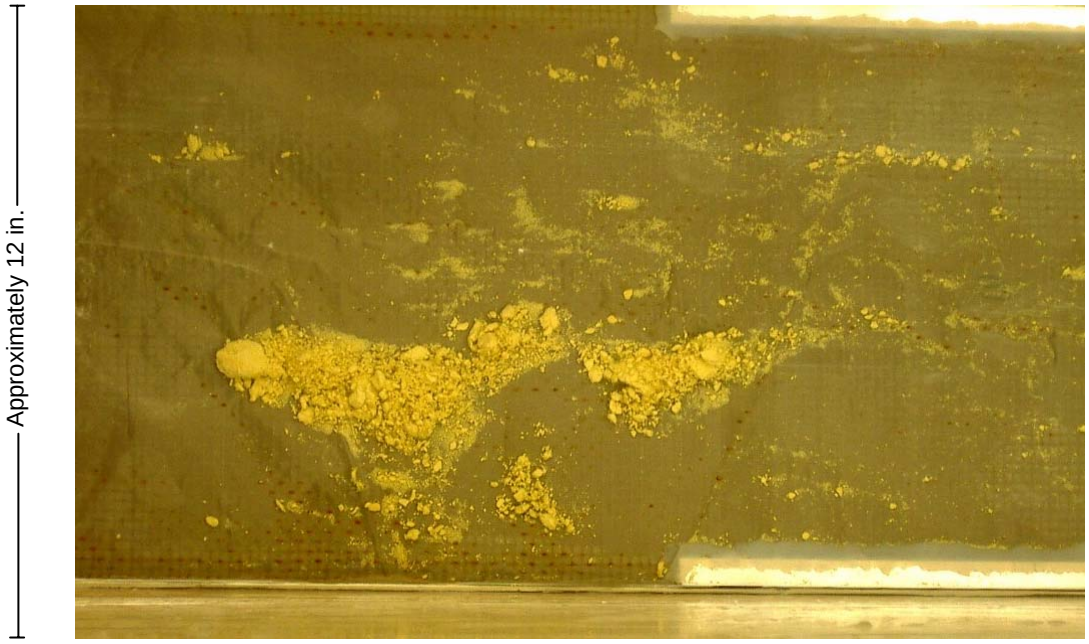

Figure 5-6. Larger clumps of CalSil remaining on the floor.

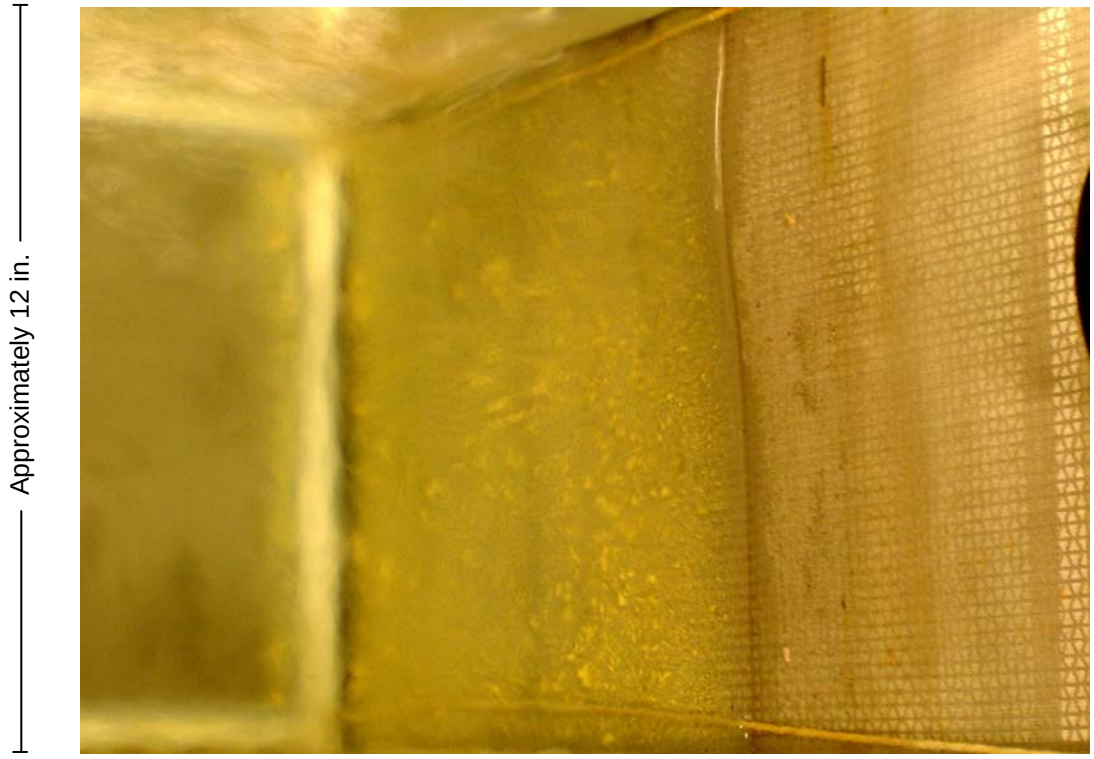

Figure 5-7. Smaller CalSil particles captured by the fine screen and the tray on the floor.

The results for the RMI debris tests are plotted according to screen size in Figures 5-8 and 5-9. For a given screen size, each plot compares the results for RMI based on the method of debris introduction and debris size. For cases where the RMI debris was introduced on the Plexiglas® floor, most of the RMI remained stationary and never reached the screen. No difference was noted in the transport of the debris on the floor between the Plexiglas® section and the test section with the tray on the floor. Any RMI debris that began to move went all the way to the test screen. The RMI began to move at a velocity of only 6.096 cm/s (0.2 ft/s), rather than move en masse. Therefore, only a small fraction of the RMI insulation passed through the screen. The measured penetration of RMI through the screen increased with increasing flow velocity because more of the RMI got to the screen; however, the majority of the RMI remained on the floor, as shown in Figure 5-10. (Note: The reflections identified in this photograph are reflected fluorescent light due to surface ripples on the water.)

For cases where the RMI debris was introduced into the flow, a significantly larger fraction went through the test screen because all of the RMI now reached the screen. For cases with RMI of the same size as the screen mesh openings, the penetration fraction ranged from 8%–22%. RMI with the aspect ratio of 4:1 [1.27 cm (1/2 in.) × 0.32 cm (1/8 in.)] demonstrated approximately the same fraction of penetration as RMI with an aspect ratio of 1:1 [0.64 cm (1/4 in.) × 0.64 cm (1/4 in.)]. It is worth noting that the water pressure did not force the RMI through the screen at any velocity. This observation is consistent with post-test observations of the RMI foils, which exhibited no flow-induced deformation. Therefore, the velocity of water was relevant only in transporting the RMI pieces to the screen.

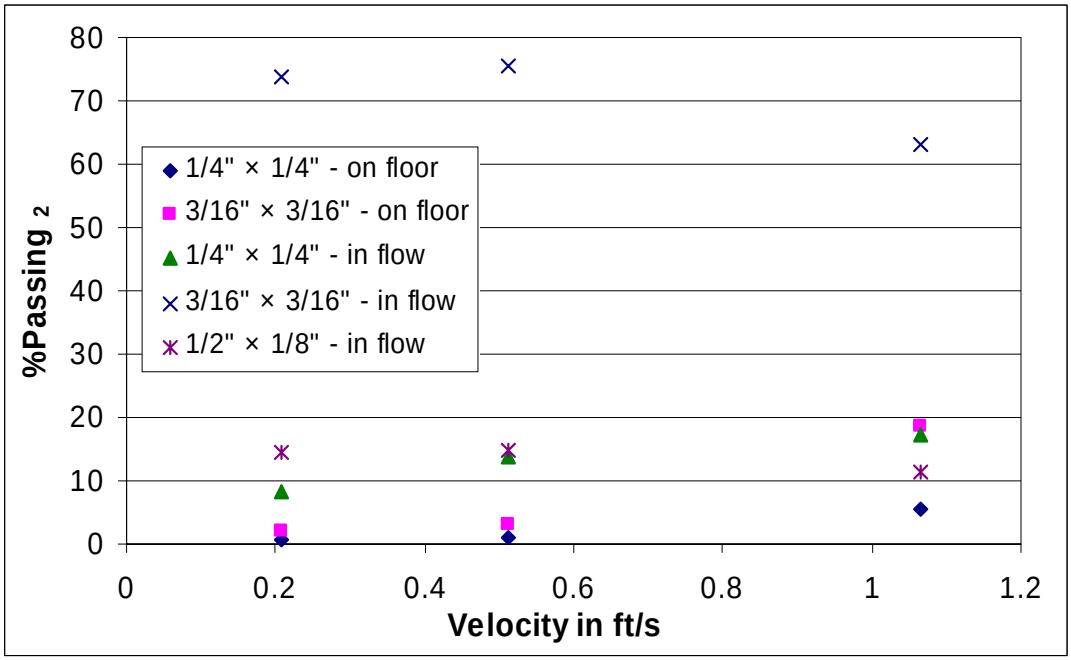

Figure 5-8. RMI—1/4-in.-Screen—%Passing$_2$ (1 ft/s = 0.305 m/s).

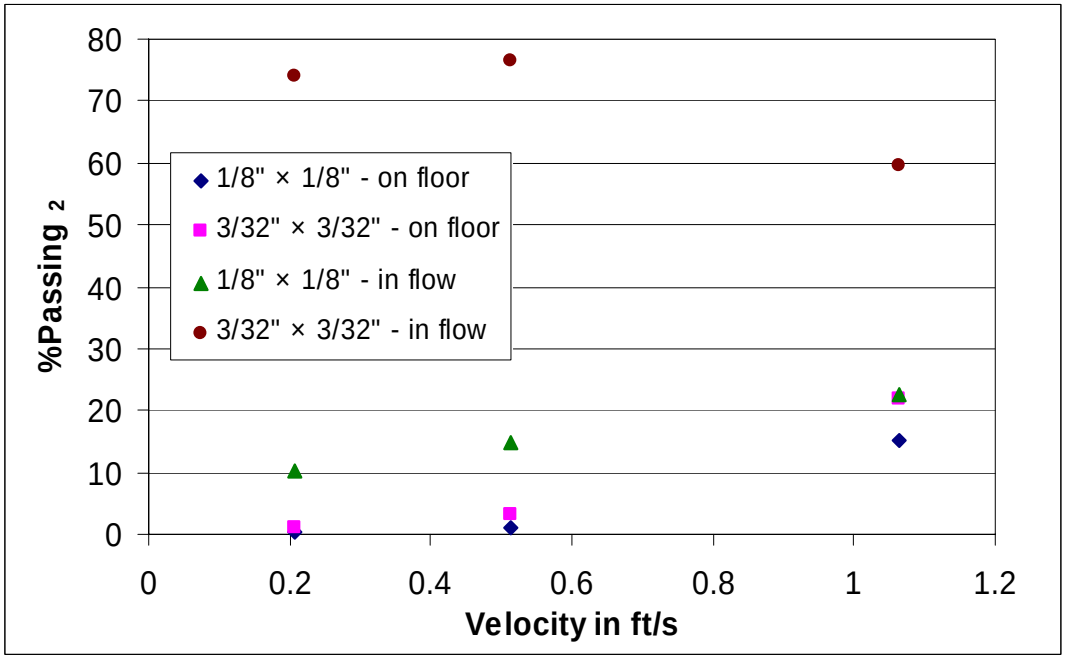

Figure 5-9. RMI—1/8-in. Screen—%Passing$_2$ (1 ft/s = 0.305 m/s).

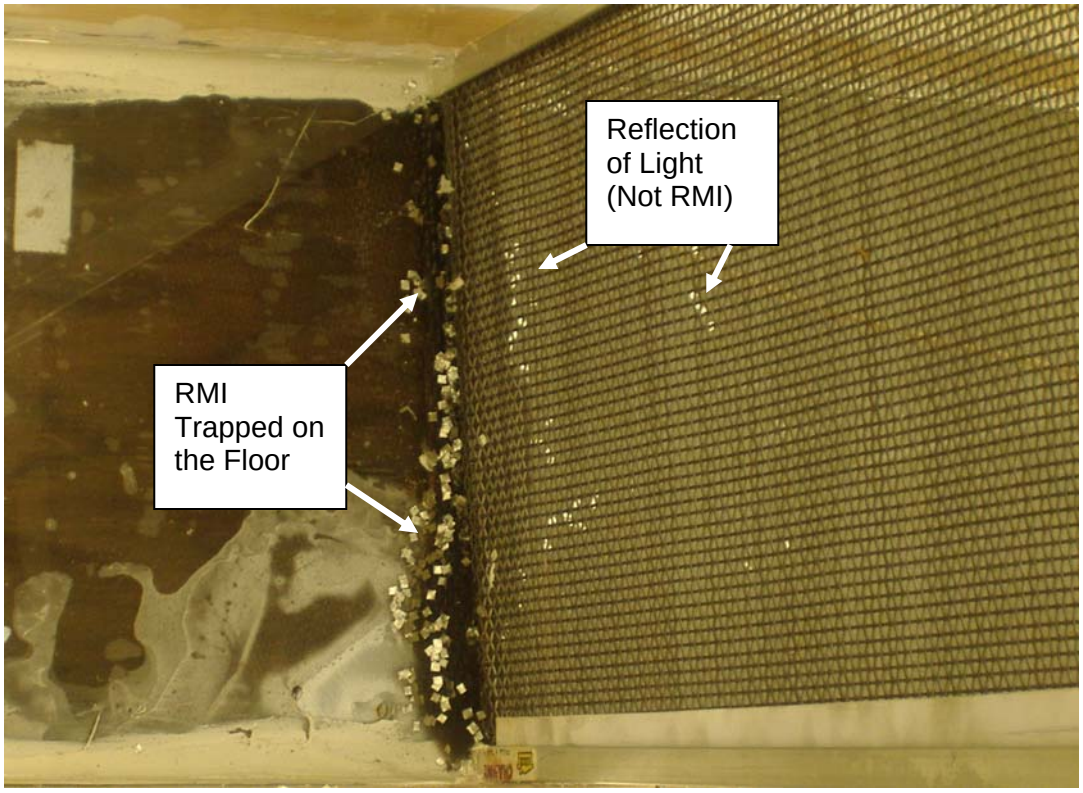

Figure 5-10. RMI at the bottom of the flume.

Figure 5-11 shows some of the RMI trapped in the screen. Consistent with expectations, some RMI particles pass through the test screen when the screen-hole size and particle size are equivalent. The maximum dimension of a square-mesh screen is the diagonal, whereas the minimum dimension of a square (or nearly square) is its edge. Because the RMI pieces were not bent by water pressure, 100% of the RMI pieces would be blocked if the largest dimension of the screen (the diagonal) were smaller than the minimum dimension of the particle (any side). That is, the screen mesh spacing would have to be 70.7% ($1/\sqrt{2}$) smaller than the particle minimum dimension to guarantee that no RMI would pass through the screen. For any screen mesh spacing relatively larger than this theoretical minimum, the penetration of particles becomes a distribution function based on relative particle dimension and particle orientation. This distribution function, if it were known, largely would describe the uncertainty among multiple, nominally replicate RMI tests. This uncertainty is much greater than the variations in screen mesh spacing and the measured RMI size distribution (Table 3-2). Conversely, as the minimum dimension of the particle approaches 70.7% of the minimum dimension of the screen, the penetration of RMI theoretically approaches 100% (slightly oversimplified). This theory is supported by the large penetration increase observed for RMI debris corresponding to 75% of the screen mesh spacing (Figures 5-8 and 5-9).

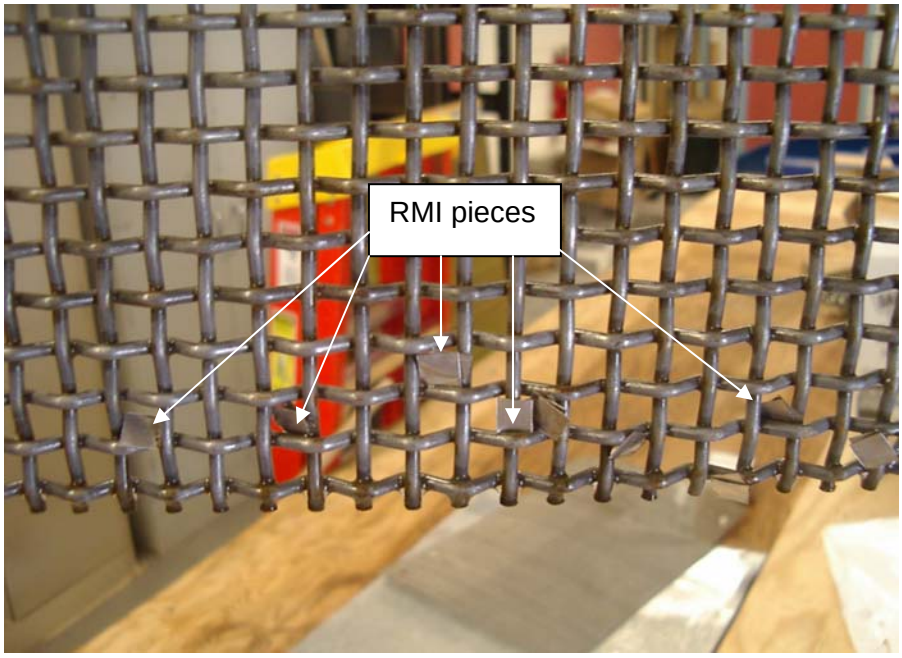

Figure 5-11. RMI lodged in the 0.64-cm (1/4-in.) screen openings.

6.0 CONCLUSIONS

It was observed that virtually all of the fine-particulate CalSil insulation passed through screen openings of any size during these tests. However, the principal factor that affected the total percentage of CalSil that passed through the screen was the amount of large clumps that remained on the floor rather than reach the screen. Higher flow velocities cause large CalSil clumps to break up, allowing more CalSil to be transported to and pass through the sump screen. Therefore, the passage of CalSil through the screen depends on the interrelationship between the size of the CalSil clumps and the flow velocity. This interdependency was not explored in these tests.

With fibrous debris (NUKON™), the fraction of debris passing through the test screen is very large (>70% in these tests) for BP NUKON™ (processed into fine fibers) as opposed to LS NUKON™. The fraction passing through each screen was <1% for LS NUKON™. The fraction of NUKON™ passing through the test screen was influenced to a much lesser extent by the velocity of flow at the screen. This observation has implications for the evaluation of the effect of post-LOCA fluids on downstream systems and components.

For RMI, the primary variables affecting test screen penetration include particle size, debris introduction method, and flow velocity. A relatively small fraction of RMI debris (<25% for any test) was observed to pass through a screen having the same screen-hole size as the RMI. However, the percentage of RMI passing through the screen increased to >60% in tests where the debris was introduced in the flow and the particle size was somewhat smaller than the screen-hole spacing. This behavior was consistent with expectations for a square particle impinging on a square mesh. As long as the minimum dimension of the impinging particle (edge) was less than the maximum dimension of the mesh (diagonal), the penetration of particles was a random function of the particle orientation arriving at the screen.

The manner in which RMI debris was introduced into the flow is also an important parameter. For debris introduced on the floor, <22% of RMI debris passed through the test screen, regardless of the debris size relative to the screen mesh spacing. For debris introduced in the flow, penetration of RMI debris smaller than the screen was ≥60% in these tests. The fraction that penetrated the screen was smaller for RMI introduced on the floor because more debris remained on the floor and did not transport to the screen during the test. The fraction of RMI that passed through the test screen also was influenced by flow velocity. Within the flow velocity range studied, higher velocities resulted in more debris penetration in tests where the RMI was introduced on the floor. When the flow velocity was <15.64 cm/s (0.513 ft/s), <4% of the RMI passed through the test screen for floor-introduced debris. However, when the velocity was 32.5 cm/s (1.065 ft/s), the penetration amount was >20% in one test.

These observations on the variables affecting the ability of RMI insulation to pass through the screen are somewhat intuitive and confirm that no unexpected phenomena occurred during these tests. For instance, water pressure did not bend larger RMI pieces and force them through the screen in any tests. Additionally, smaller RMI mostly passed through the screens if the pieces were initially transported and did not get caught in the screen wires. A great deal of variability was observed in these tests, which was expected. Variability among results for somewhat similar tests is governed largely by the random orientation of the debris arriving at the screen and not by uncertainties associated with the screen mesh spacing and RMI size distribution variability. More accurate quantification of this variability was outside the scope of this effort.

Page intentionally left blank

REFERENCES

1. D. V. Rao, B. C. Letellier, A. K. Maji, and B. Marshall, "GSI-191: Separate-Effects Characterization of Debris Transport in Water," United States Nuclear Regulatory Commission report NUREG/CR-6772 (August 2002), Los Alamos National Laboratory report LA-UR-01-6882 (December 2001).

2. Rao, D. V.; Shaffer, C. J.; Letellier, B. C.; Maji, A.; Bartlein, L., "GSI-191: Integrated Debris-Transport in Water Using Simulated Containment Floor Geometries," Los Alamos National Laboratory report LA-UR-02-6786, NUREG/CR-6773 (2002).

3. Shaffer, C. J.; Leonard, M. T.; Maji, A.; Ghosh, A.; Letellier, B.; Chang, T. Y., "Debris Accumulation and Head-Loss Data for Evaluating the Performance of Vertical Pressurized-Water-Reactor Recirculation Sump Screens," Los Alamos National Laboratory report LA-UR-03-9269 (2004).

4. Rao, D. V., Letellier, B. C., Ross, K. W., Bartlein, L. S., and Leonard, M. T., "GSI-191 Technical Assessment: Summary and Analysis of U. S. Pressurized Water Reactor Industry Survey Responses and Responses to GL 97-04," Los Alamos National Laboratory report LA-UR-01-1800 (August 2002), NUREG/CR-6762, Vol.2.

5. F. W. Sciacca and D. V. Rao, "Reassessment of Debris-Ingestion Effects on Emergency-Core-Cooling-System Pump Performance," Proceedings of the NRC/NEA International Workshop, Albuquerque, New Mexico (February 2004).

6. C. J. Shaffer, D. V. Rao, M. T. Leonard, and K. W. Ross, "Knowledge Base for the Effect of Debris on Pressurized Water Reactor Emergency Core Cooling Sump Performance," United States Nuclear Regulatory Commission report NUREG/CR-6808, Los Alamos National Laboratory report LA-UR-03-0880 (February 2003).

7. D. V. Rao, C. J. Shaffer, and S. G. Ashbaugh, "GSI-191: Technical Assessment: Development of Debris Generation Quantities in Support of the Parametric Evaluation," United States Nuclear Regulatory Commission report NUREG/CR-6762, Vol. 3 (2002), Los Alamos National Laboratory report LA-UR-01-6640 (2001).

8. M. T. Leonard, C. J. Shaffer, D. V. Rao, A. K. Maji, and A. Ghosh, "GSI-191: Experimental Studies of Loss-of-Coolant-Accident-Generated Debris Accumulation and Head Loss with Emphasis on the Effects of Calcium Silicate Insulation," Los Alamos National Laboratory report LA-UR-04-1227 (April 2004).

9. M. Marshall, "Generic Safety Issue 191 Overview of Study and Overview of Results," presentation to a public meeting, Rockville, Maryland, July 26–27, 2001, p. 17.

Page intentionally left blank